NANO LETTERS

pubs.acs.org/NanoLett Letter

Modulation Doping of Single-Layer Semiconductors for Improved Contact at Metal Interfaces

Yeonchoo Cho,* Gabriel R. Schleder, Daniel T. Larson, Elise Brutschea, Kyung-Eun Byun, Hongkun Park, Philip Kim, and Efthimios Kaxiras

Cite This: *Nano Lett.* 2022, 22, 9700−9706 Read Online

ACCESS | Metrics & More | Article Recommendations | Supporting Information

ABSTRACT: Single layers of two-dimensional (2D) materials hold the promise for further miniaturization of semiconductor electronic devices. However, the metal−semiconductor contact resistance limits device performance. To mitigate this problem, we propose modulation doping, specifically a doping layer placed on the opposite side of a metal−semiconductor interface. Using first-principles calculations to obtain the band alignment, we show that the Schottky barrier height and, consequently, the contact resistance at the metal−semiconductor interface can be reduced by modulation doping. We demonstrate the feasibility of this approach for a single-layer tungsten diselenide (WSe_2) channel and 2D MXene modulation doping layers, interfaced with several different metal contacts. Our results indicate that the Fermi level of the metal can be shifted across the entire band gap. This approach can be straight-forwardly generalized for other 2D semiconductors and a wide variety of doping layers.

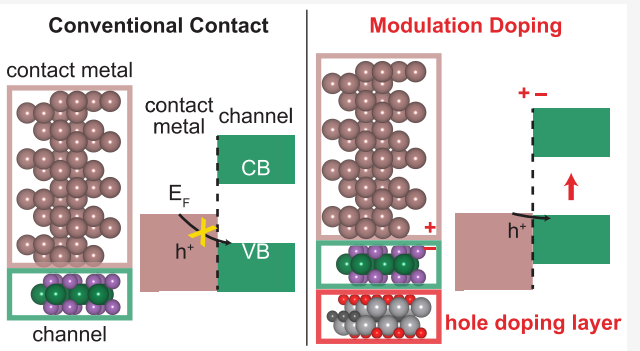

KEYWORDS: *Contact, modulation doping, metal−semiconductor interface, density functional theory, Schottky barrier*

Electronic devices based on layered semiconductors have been gaining increased attention in both industrial applications and basic research. In the semiconductor industry, the 2D nature of these materials is expected to allow further miniaturization of transistors.[1,2] 2D semiconductor heterostructures have also been adopted to study emergent quantum phenomena arising at the van der Waals interface.[3] However, high contact resistance continues to be a significant problem for the use of 2D materials in both industrial applications and fundamental research.[4] High contact resistance slows circuit operation, increases power consumption, generates unnecessary heat, and reduces the on−off ratio. Similarly, high contact resistance makes measurements of linear response transport coefficients, such as the Hall density, more challenging. At low temperatures, where most quantum transport measurements are performed, a finite Schottky barrier critically prohibits low energy carrier injection.

Reducing the contact resistance in 2D materials has motivated numerous experimental and theoretical studies. One common approach is to manipulate the metal−semiconductor interface in order to reduce the number of metal-induced gap states (MIGS) that lead to Fermi-level pinning.[5,6] Using a semimetal as the contact reduces the number of MIGS due to the low density of states (DOS) near the Fermi level of the semimetal contact.[7] Insertion of another layered material between the metal and semiconductor was theoretically predicted to reduce MIGS,[8] and it was experimentally verified using hexagonal boron nitride (hBN) inserted between gold and MoS_2.[9] Also, producing ultraclean van der Waals contacts through careful device fabrication appears to leave the Fermi level unpinned.[10,11] Another approach to reducing contact resistance is through doping.[12] Doping makes the Schottky barrier thinner so that the contact resistance is reduced by enhanced tunneling.[13] In addition, the ultimate limit of contact resistance is governed by the density of states near the Fermi level, controlled by carrier density and doping.[14] Substitutional doping is a standard approach for silicon, but for 2D semiconductors, such as Nb in MoS_2, it has not produced the same effect due to undesired defect formation and insufficient dielectric screening.[15] Electrostatic doping is theoretically well-motivated and widely used experimentally,[16] but the electrostatically induced carrier density is limited by dielectric breakdown.

We will focus instead on modulation doping to control the Schottky barrier height (SBH). Modulation doping refers to

Received: October 12, 2022
Revised: November 19, 2022
Published: November 28, 2022

https://doi.org/10.1021/acs.nanolett.2c04011
Nano Lett. 2022, 22, 9700−9706

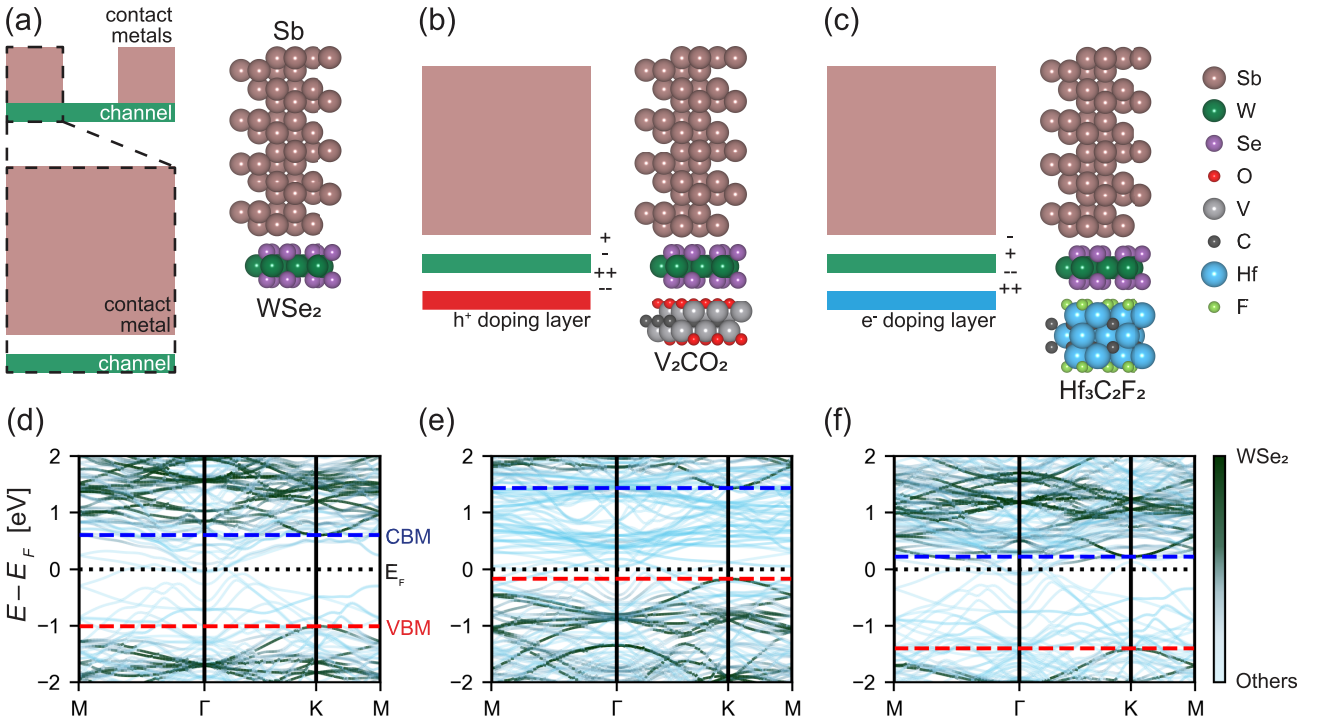

Figure 1. Schematics, atomic structures, and band diagrams to demonstrate the modulation doping concept. Schematics and atomic structures of (a) conventional metal contact on the 2D semiconductor; (b) hole-doping layer added to the contact to reduce the hole SBH; (c) electron-doping layer added to the contact to reduce the electron SBH. The inset of (a) shows the source, drain, and channel of a 2D channel-based transistor. Here, the contact metal is Sb, the 2D semiconductor is WSe_2, the hole-doping layer is V_2CO_2, and the electron-doping layer is $Hf_3C_2F_2$. The color coding for different elements is shown on the right. (d–f) are the corresponding band structures. Red and blue dashed lines indicate the valence band maximum and the conduction band minimum of WSe_2, respectively. The color scale represents the contribution of WSe_2 in each state, as indicated by the color bar on the right.

doping provided by a separate proximal layer. It has been utilized mainly in GaAs-based systems to achieve a high carrier mobility.[17] Among 2D materials, modulation doping achieved a record-high carrier density (3×10^{13} cm^{-2}) in graphene using α-ruthenium(III) chloride as the doping layer.[18] This level of doping is difficult to achieve with conventional electrostatic doping in practice due to dielectric breakdown. Similarly, the use of defects in a BN layer has been proposed based on DFT calculations.[19] Note that the contact resistance of a 2D transistor can be divided into two parts: the interface between the contact metal and the 2D semiconductor, and the virtual interface within the semiconductor between the portion in contact with the metal and the portion in the channel.[4,20] Doping in the channel region can reduce the latter part of the contact resistance,[21−24] but such channel doping does not directly affect the former part of the contact resistance. A few reports studied the doping effect from a substrate,[25−27] but none have focused on the modulation doping effect solely to a metal−semiconductor interface.

In this study, we show that a modulation doping layer added on the opposite side of a metal−semiconductor interface can shift the band alignment between the contact metal and the semiconductor, which we take to be a single-layer transition metal dichalcogenide (TMD). The fact that the TMD layer is extremely thin makes it possible to modify the dipole generated at the metal/TMD interface by such doping. Since our modulation doping approach, as opposed to, e.g., the insertion approach, does not manipulate the metal/TMD interface itself, MIGS still exist, but they can be reduced by combining our approach with the insertion approach. In this way, the Fermi level can be shifted across the entire band gap of the semiconductor, thus reducing the Schottky barrier height and the contact resistance.

Modulation doping in the contact region. If a 2D material is employed as the channel material, its thinness allows another layer, placed below the channel, to help control the device characteristics. We study a modulation doping layer placed in the contact region in order to improve the contact behavior, as shown schematically in Figure 1(a). To demonstrate this idea, we use tungsten diselenide (WSe_2) as the semiconducting channel material and two different types of MXenes as doping layers, for positive (hole) and negative (electron) doping. MXenes are a broad class of layered materials derived by etching out the A layers from bulk MAX phase crystals that can be readily produced in the lab.[28] MXenes are suitable for modulation doping of 2D materials due to their two-dimensional nature, which reduces the possibility of chemical bond formation and surface roughness, and due to their wide range of work functions.[29] We chose oxygen-terminated vanadium carbide (V_2CO_2)[30] and fluorine-terminated hafnium carbide ($Hf_3C_2F_2$)[31] for this study because their work functions are 7.0 and 3.2 eV, respectively, which are higher (lower) than the ionization potential (electron affinity) of WSe_2. Thus, V_2CO_2 is capable of hole-doping WSe_2, while $Hf_3C_2F_2$ can serve as an electron donor, as shown by the location of the Fermi level in the band structures in Figures S2 and S3. Since these materials are experimentally available, the practical realization of these heterostructures is in principle possible, but the process should be carefully optimized because of the (electro-)chemical activity of these materials. Our task is

https://doi.org/10.1021/acs.nanolett.2c04011
Nano Lett. 2022, 22, 9700−9706

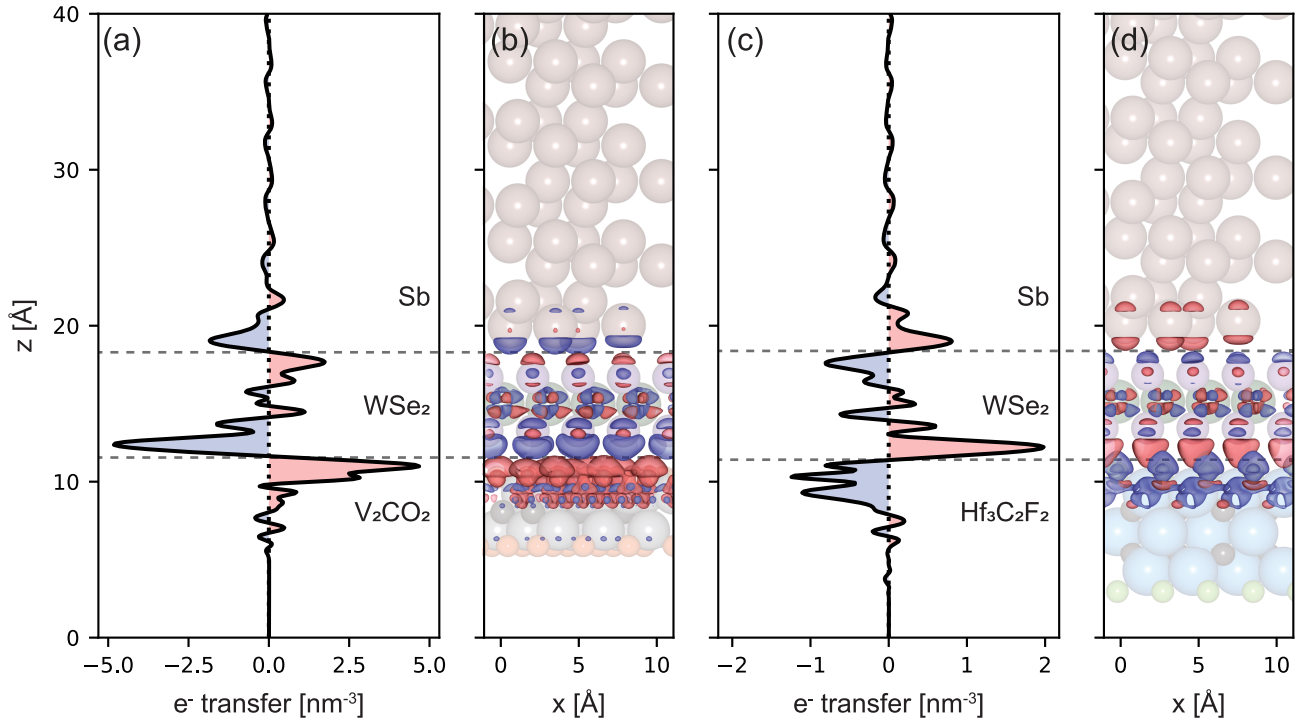

Figure 2. Electron redistribution caused by the attachment of a modulation doping layer. In (a,b), the modulation doping layer is V_2CO_2 (hole doping), and in (c,d), it is $Hf_3C_2F_2$ (electron doping). In (b,d), charge density difference isosurfaces are superimposed on the atomic structure. Blue (red) shades and surfaces represent electron deficit (excess), which is shown quantitatively by the black curve in (a,c), in units of the number of charges per length and per area. The color of each element is the same as in Figure 1. The horizontal gray dashed lines indicate the positions of interfaces between different materials.

to determine how band alignment at the interface between the metal (contact) and semiconductor (channel) can be modified by modulation doping layers. Computational details are in the Supporting Information.

We first show that modulation doping enables a significant shift in the band alignment at the metal/TMD interface. Figure 1 shows the location of the Fermi level relative to the WSe_2 band gap when WSe_2 is in contact with Sb, with and without one of the MXene doping layers on the opposite side. The Fermi level is determined by the metal layer, as verified by calculating the work function of the combined structures. It can also be seen by comparing panels (d) and (f) in Figure 1, where the Fermi level maintains the same relation to the metal bands (light blue) both with and without a doping layer. However, the band alignment of WSe_2 shifts dramatically due to the modulation doping. In the presence of V_2CO_2 (hole doping), the VBM lies just below the Fermi level. On the other hand, in the presence of $Hf_3C_2F_2$ (electron doping), the CBM is just above the Fermi level. Since the Fermi level is determined by the contact metal, the energetic distance between the Fermi level and the conduction band minimum corresponds to the electron SBH. Similarly, the hole SBH is the energy distance between the Fermi level and the valence band maximum. Thus, by changing the modulation doping layer, the relative position of the Fermi level can be shifted across almost the full band gap of WSe_2, and the SBH can be reduced for either hole or electron doping. Note that the size of the WSe_2 band gap barely changes and its band edges do not hybridize with the metal bands, implying that modulation doping rigidly shifts the bands of WSe_2, so its transport properties should not be compromised. In particular, we do not expect additional resistance within the semiconductor at the interface between the region in contact with the metal and the channel region.[4,20]

Origin and magnitude of band alignment shift. The change in band alignment is due to electronic charge redistribution caused by the modulation doping layer. In Figure 2, we plot the planar average of the charge density difference and corresponding isosurfaces of that difference. The largest amount of charge redistribution occurs at the interface between the WSe_2 layer and the doping layer. Since V_2CO_2 has states that can accept electrons from WSe_2, the V_2CO_2 layer draws electrons away from the WSe_2 layer. On the other hand, $Hf_3C_2F_2$ donates electrons to WSe_2. Perhaps more important, though smaller in size, is the charge redistribution at the interface between the Sb metal and the WSe_2 layer that changes the dipole moment at the Sb/WSe_2 interface, resulting in the band alignment shift. This charge redistribution is schematically indicated with + and − signs in Figure 1(b,c).

The charge density redistribution is larger in the case of V_2CO_2, due to the larger difference between the work function of V_2CO_2 and the ionization potential of WSe_2, compared to the difference between the work function of $Hf_3C_2F_2$ and the electron affinity of WSe_2. The larger difference means more charge moves to form the interface dipole that equalizes the Fermi level. Note that the charge density changes are mainly in *p* orbitals of Se and *d* orbitals of W, which constitute the MIGS shown in Figure S4. Therefore, the electronic charge redistribution can be regarded as filling or emptying MIGS with additional charge redistribution to compensate for the electrostatic changes.

MIGS can be seen in plots of the projected density of states (PDOS). Figure 3(a) shows the DOS of the metal/WSe_2 system, projected onto the WSe_2 layer, for three different

https://doi.org/10.1021/acs.nanolett.2c04011
Nano Lett. 2022, 22, 9700−9706

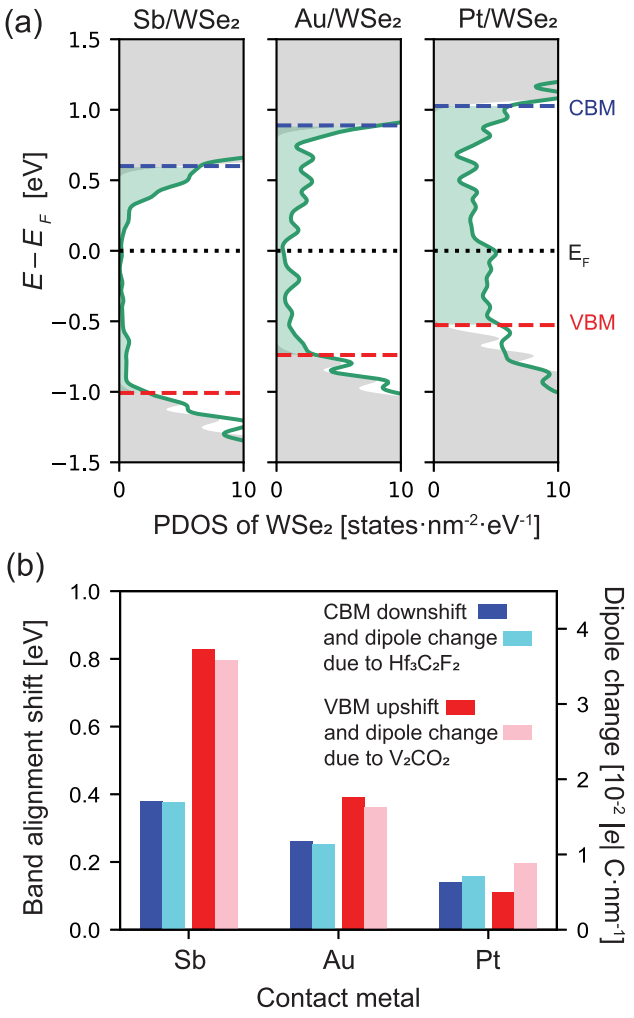

Figure 3. Metal-induced gap states and alignment shifts for various metals. (a) Projected density of states of WSe_2 in the M/WSe_2 heterostructure (M = Sb, Au, and Pt). Green shades represent metal-induced gap states formed within the band gap of WSe_2. The blue and red dashed lines represent the WSe_2 conduction band minimum and valence band maximum, respectively. Gray shades are the total density of states of isolated WSe_2 as a reference. (b) The effect of contact electrode material on the band alignment shift and the M/WSe_2 interfacial dipole. Refer to Figure S5 for atomic structures and band structures.

metals. We used gold (Au), antimony (Sb), and platinum (Pt) as representative *s*-, *p*-, and *d*-valence metals. If the metal were not present, there would be no states between the VBM and CBM, as shown in gray shades, but the presence of the metal gives rise to a nonzero DOS in the gap. Sb generates the fewest MIGS, due to its semimetallic nature.[7] Pt generates the most MIGS, since its valence *d* orbitals hybridize well with W *d* orbitals.[32] Figure 3(b) shows the magnitude of the band alignment shift and the metal/WSe_2 interfacial dipole change due to the two modulation doping layers for the same three metals. It is clear that the magnitude of the band alignment shift correlates well with the metal/WSe_2 interfacial dipole change. This is expected, since the band alignment shift is caused by the change in the interfacial dipole at the metal/TMD interface due to the doping layer. Note that the size of the shift is inversely related to the number of MIGS. MIGS, being metallic in nature, can accommodate charges and screen the electrostatic change at the interface between WSe_2 and a modulation doping layer. Therefore, when there are more MIGS, more charges can be screened at the TMD layer where MIGS are located, resulting in more charge redistribution at the TMD/doping layer interface, less charge redistribution at the metal/TMD interface, and a smaller shift in the band alignment.

We chose Sb as the contact metal in Figure 1 because it generates the fewest MIGS and thus demonstrates the shift in the band alignment most clearly. However, the band alignment shift is still significant for other contact metals, despite the strong Fermi-level pinning tendency of TMDs.[32] Note that fewer than 0.5 electrons/nm^2 are necessary for a V_2CO_2 layer to make a upward WSe_2 band shift by 0.8 eV. Thus, modulation doping using more conventional materials like insulators with point defects, instead of metallic MXenes, can also yield a noticeable band alignment shift.

Combining with the insertion layers. Since the doping layer is located on the side opposite to the metal−semiconductor interface, our modulation doping approach can be combined with well-known insertion approaches[6] that modify the metal−semiconductor interface. For example, if modulation doping is combined with a hexagonal boron nitride (hBN) insertion layer, a very low electron SBH to WSe_2 can be achieved (Figure 4). Graphene or hBN insertion is a theoretically motivated and experimentally demonstrated technique for reducing the electron SBH.[8,9] The inserted layer plays two roles: it reduces the work function of the metal surface (particularly effective in Co), and it also reduces the formation of MIGS, as can be seen by comparing panels (d) and (e) of Figure 4, where the PDOS in the gap is noticeably reduced. Although near-zero electron SBH to MoS_2 was reported with hBN insertion,[9] there is a finite electron SBH to WSe_2, since the electron affinity of WSe_2 is lower than that of MoS_2. However, including modulation doping in addition to hBN insertion can reduce the electron SBH close to zero, as shown in Figure 4(f). Figure S6 shows that in the case of $MoSe_2$, the electron SBH can be reduced to zero by combining hBN insertion and modulation doping, owing to its higher electron affinity compared to WSe_2.

An interesting variation of the insertion approach is shown in Figure 5(a). If, instead of a single-layer semiconducting TMD, we place a bilayer in contact with the metal, it behaves much like the single layer of our previous discussion with a MIGS-reducing insertion layer that happens to be the same material. Due to the electric field generated by a doping layer, the band alignment is different in the two layers, as shown in Figure 5(b). The layer far from the metal−TMD interface is doped more, due to the proximity of the doping layer and the insulation provided by the layer closer to the interface. This effect leads to the zero hole SBH even when Pt, with its multitude of MIGS, is used as the contact metal. (The Sb case is shown in Figure S7.) If the contact geometry shown in the inset of Figure 5 is realized, barrier-less injection of holes can be achieved with many metals. Thus, the metal contact to a WSe_2 bilayer can be viewed as the insertion of a WSe_2 layer to control the SBH. Since layer-by-layer etching of TMDs has already been reported,[33,34] this geometry can be realized, and it has the benefit of reducing the number of different materials needed in the contact, since the insertion layer and the channel material are the same.

Note that the band shift at the metal−semiconductor interface is smaller than in the case of the single layer. This is even more dramatic for the case of Sb, as shown in Figure S7.

https://doi.org/10.1021/acs.nanolett.2c04011
Nano Lett. 2022, 22, 9700−9706

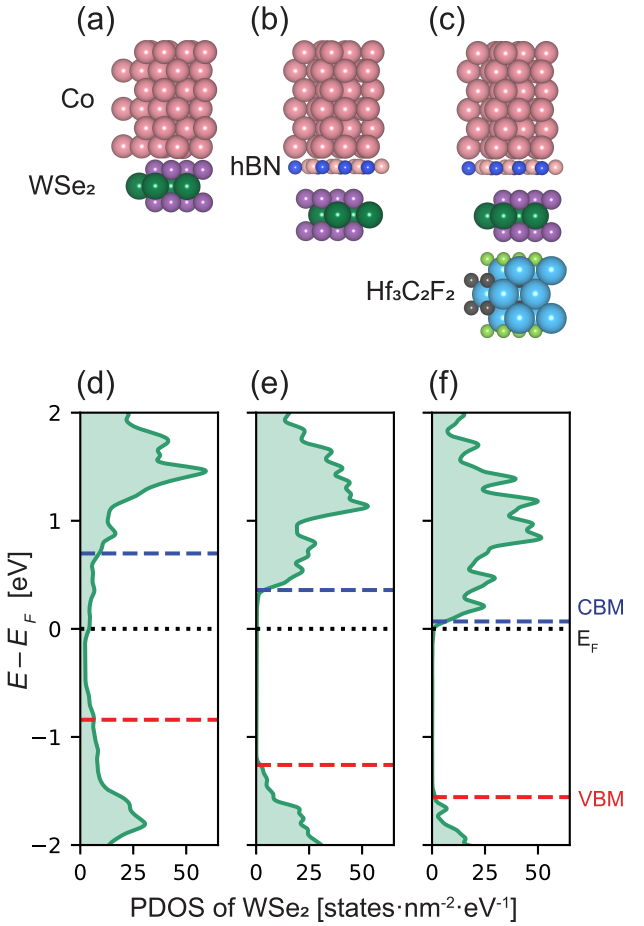

Figure 4. Synergy of modulation doping and insertion. Atomic structures (a–c) and corresponding projected densities of states (PDOS) (d–f) of WSe_2 in Co/WSe_2, Co/hBN/WSe_2, and Co/hBN/WSe_2/$Hf_3C_2F_2$ heterostructures, respectively. The blue and red dashed lines represent the conduction band minimum and the valence band maximum, respectively. The black dotted lines represent the Fermi level, which is set by the contact metal Co in all cases.

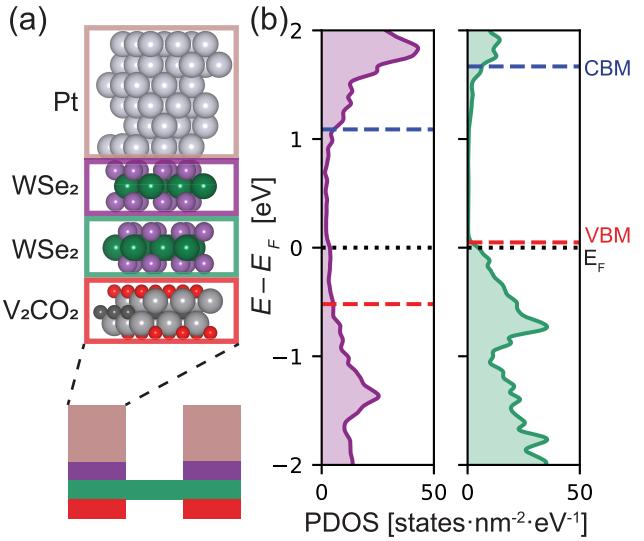

Figure 5. Special case of the insertion approach using a bilayer. (a) Atomic structure of the Pt/WSe_2 bilayer/V_2CO_2 heterostructure. Inset at the bottom indicates a possible implementation of this heterostructure. (b) Projected density of states (PDOS) of WSe_2 in the heterostructure. Green and purple curves in (b) show the PDOS of the layers indicated by the green and purple rectangles in (a). The blue and red dashed lines represent the conduction band minimum and the valence band maximum, respectively.

When a single layer of WSe_2 contacts Sb, its VBM is positioned 0.17 eV below the Fermi level. On the other hand, when Sb contacts bilayer WSe_2, the VBM of the layer adjacent to Sb lies 0.58 eV below the Fermi level. This is expected because the screening by the bilayer is stronger than that by the single layer, reducing the charge redistribution at the metal–semiconductor interface.

Extending the modulation doping approach. Since our approach only relies on the incomplete screening of a semiconductor, it will be effective for any layered semiconductor. We have already shown that our approach can be used to reduce the electron SBH of a $MoSe_2$ transistor (Figure S6). The electron SBH to MoS_2, another commonly used 2D semiconductor, will be easier to manipulate, since its electron affinity is higher. The main limitation of nonlayered materials is that the atomic structure and, as a consequence, the transport properties might be vastly different from the bulk if the nonlayered material is made thin enough for modulation doping to be effective.

There is significant flexibility in choosing the doping material. The only essential requirement is either a high (low) enough work function for hole (electron) doping. We have demonstrated the feasibility of this approach using MXenes as the doping material. However, since the density of MIGS is comparable to the point defect density in insulators, a more conventional insulator-based modulation doping approach is also expected to yield a noticeable band alignment shift. This study focused on the feasibility of a modulation doping framework with several different contact metals. The effect of different 2D semiconducting materials and doping materials will be a subject of further studies.

Even though this approach of controlling the SBH has not been explicitly reported in the literature yet, there are experimental observations indicating that the physics behind modulation doping plays a role at the contact. For example, Shen et al.[7] used a SiN_x substrate in devices that displayed a contact resisitance between Sb and TMDs close to the quantum limit. The electron affinity of silicon nitride is ∼2 eV. Therefore, shallow levels in SiN_x can play a role in electron doping, reducing the electron SBH.[35] In a recent report by Wang et al.,[11] the n-type SiO_2 substrate was passivated to prevent the doping effect in order to allow hole transport through the channel. In these studies, the substrate affected the channel region as well as the contact region, so a further study is needed to separate the effects of the substrate in the two regions.

Conclusion. We have shown that modulation doping is an effective method to control the Schottky barrier height and, as a consequence, the contact resistance between a metal and a single-layer semiconductor. A doping layer added to the side opposite to the metal–semiconductor interface can shift the band alignment at the metal–semiconductor interface. This shift is possible due to the incomplete screening by single-layer semiconductors. This modulation doping approach is a new and general technique that can be combined with other approaches for controlling the Schottky barrier height.

https://doi.org/10.1021/acs.nanolett.2c04011
Nano Lett. 2022, 22, 9700–9706

■ ASSOCIATED CONTENT

Supporting Information

The Supporting Information is available free of charge at https://pubs.acs.org/doi/10.1021/acs.nanolett.2c04011.

Methods, supercell descriptions, and figures showing additional atomic structures and their electronic properties (PDF)

■ AUTHOR INFORMATION

Corresponding Author

Yeonchoo Cho − *Samsung Advanced Institute of Technology, Samsung Electronics, Suwon 16678, Republic of Korea; Department of Physics, Harvard University, Cambridge, Massachusetts 02138, United States;* orcid.org/0000-0002-8578-2608; Email: ycho1@g.harvard.edu

Authors

Gabriel R. Schleder − *John A. Paulson School of Engineering and Applied Sciences, Harvard University, Cambridge, Massachusetts 02138, United States;* orcid.org/0000-0003-3129-8682

Daniel T. Larson − *Department of Physics, Harvard University, Cambridge, Massachusetts 02138, United States;* orcid.org/0000-0001-8528-0280

Elise Brutschea − *Department of Chemistry and Chemical Biology, Harvard University, Cambridge, Massachusetts 02138, United States*

Kyung-Eun Byun − *Samsung Advanced Institute of Technology, Samsung Electronics, Suwon 16678, Republic of Korea*

Hongkun Park − *Department of Chemistry and Chemical Biology and Department of Physics, Harvard University, Cambridge, Massachusetts 02138, United States;* orcid.org/0000-0001-9576-8829

Philip Kim − *Department of Physics, Harvard University, Cambridge, Massachusetts 02138, United States;* orcid.org/0000-0002-8255-0086

Efthimios Kaxiras − *John A. Paulson School of Engineering and Applied Sciences and Department of Physics, Harvard University, Cambridge, Massachusetts 02138, United States*

Complete contact information is available at: https://pubs.acs.org/10.1021/acs.nanolett.2c04011

Notes

The authors declare no competing financial interest.

■ ACKNOWLEDGMENTS

This work was funded by the STC Center for Integrated Quantum Materials, NSF Grant No. DMR-1231319; NSF Award No. DMR-1922172; NSF Fellowship DGE-1745303; the Army Research Office under Cooperative Agreement Number W911NF-21-2-0147; Harvard FASRC; and Samsung Advanced Institute of Technology (IO211105-09093-01).

■ REFERENCES

(1) Liu, Y.; Duan, X.; Shin, H.-J.; Park, S.; Huang, Y.; Duan, X. Promises and prospects of two-dimensional transistors. *Nature* **2021**, *591*, 43−53.

(2) Su, S.-K.; Chuu, C.-P.; Li, M.-Y.; Cheng, C.-C.; Wong, H.-S. P.; Li, L.-J. Layered Semiconducting 2D Materials for Future Transistor Applications. *Small Struct.* **2021**, *2*, 2000103.

(3) Wilson, N. P.; Yao, W.; Shan, J.; Xu, X. Excitons and emergent quantum phenomena in stacked 2D semiconductors. *Nature* **2021**, *599*, 383−392.

(4) Allain, A.; Kang, J.; Banerjee, K.; Kis, A. Electrical contacts to two-dimensional semiconductors. *Nat. Mater.* **2015**, *14*, 1195−1205.

(5) Tersoff, J. Schottky Barrier Heights and the Continuum of Gap States. *Phys. Rev. Lett.* **1984**, *52*, 465−468.

(6) Tung, R. The physics and chemistry of the Schottky barrier height. *Appl. Phys. Rev.* **2014**, *1*, 011304.

(7) Shen, P.-C.; Su, C.; Lin, Y.; Chou, A.-S.; Cheng, C.-C.; Park, J.-H.; Chiu, M.-H.; Lu, A.-Y.; Tang, H.-L.; Tavakoli, M. M.; et al. Ultralow contact resistance between semimetal and monolayer semiconductors. *Nature* **2021**, *593*, 211−217.

(8) Farmanbar, M.; Brocks, G. Ohmic Contacts to 2D Semiconductors through van der Waals Bonding. *Adv. Electron. Mater.* **2016**, *2*, 1500405.

(9) Cui, X.; Shih, E.-M.; Jauregui, L. A.; Chae, S. H.; Kim, Y. D.; Li, B.; Seo, D.; Pistunova, K.; Yin, J.; Park, J.-H.; et al. Low-temperature ohmic contact to monolayer MoS_2 by van der Waals bonded Co/*h*-BN electrodes. *Nano Lett.* **2017**, *17*, 4781−4786.

(10) Wang, Y.; Kim, J. C.; Wu, R. J.; Martinez, J.; Song, X.; Yang, J.; Zhao, F.; Mkhoyan, A.; Jeong, H. Y.; Chhowalla, M. Van der Waals contacts between three-dimensional metals and two-dimensional semiconductors. *Nature* **2019**, *568*, 70−74.

(11) Wang, Y.; Kim, J. C.; Li, Y.; Ma, K. Y.; Hong, S.; Kim, M.; Shin, H. S.; Jeong, H. Y.; Chhowalla, M. P-type electrical contacts for two-dimensional transition metal dichalcogenides. *Nature* **2022**, *610*, 61−66.

(12) Zheng, Y.; Gao, J.; Han, C.; Chen, W. Ohmic Contact Engineering for Two-Dimensional Materials. *Cell Rep. Phys. Sci.* **2021**, *2*, 100298.

(13) Sze, S. M.; Ng, K. K. *Physics of Semiconductor Devices*, 3rd ed.; Wiley-Interscience, 2006.

(14) Jena, D.; Banerjee, K.; Xing, G. H. Intimate contacts. *Nat. Mater.* **2014**, *13*, 1076−1078.

(15) Gao, H.; Suh, J.; Cao, M. C.; Joe, A. Y.; Mujid, F.; Lee, K.-H.; Xie, S.; Poddar, P.; Lee, J.-U.; Kang, K.; Kim, P.; Muller, D. A.; Park, J. Tuning Electrical Conductance of MoS_2 Monolayers through Substitutional Doping. *Nano Lett.* **2020**, *20*, 4095−4101.

(16) Padilha, J.; Fazzio, A.; da Silva, A. J. R. van der Waals Heterostructure of Phosphorene and Graphene: Tuning the Schottky Barrier and Doping by Electrostatic Gating. *Phys. Rev. Lett.* **2015**, *114*, 066803.

(17) Nguyen, L.; Larson, L.; Mishra, U. Ultra-high speed modulation-doped field-effect transistors: a tutorial review. *Proc. IEEE* **1992**, *80*, 494−518.

(18) Wang, Y.; et al. Modulation Doping via a Two-Dimensional Atomic Crystalline Acceptor. *Nano Lett.* **2020**, *20*, 8446−8452.

(19) Wang, D.; Li, X.-B.; Sun, H.-B. Modulation Doping: A Strategy for 2D Materials Electronics. *Nano Lett.* **2021**, *21*, 6298−6303.

(20) Somvanshi, D.; Kallatt, S.; Venkatesh, C.; Nair, S.; Gupta, G.; Anthony, J. K.; Karmakar, D.; Majumdar, K. Nature of carrier injection in metal/2D-semiconductor interface and its implications for the limits of contact resistance. *Phys. Rev. B* **2017**, *96*, 205423.

(21) Arnold, A. J.; Schulman, D. S.; Das, S. Thickness Trends of Electron and Hole Conduction and Contact Carrier Injection in Surface Charge Transfer Doped 2D Field Effect Transistors. *ACS Nano* **2020**, *14*, 13557−13568.

(22) McClellan, C. J.; Yalon, E.; Smithe, K. K. H.; Suryavanshi, S. V.; Pop, E. High Current Density in Monolayer MoS_2 Doped by AlO_x. *ACS Nano* **2021**, *15*, 1587−1596.

(23) Lee, D.; Lee, J. J.; Kim, Y. S.; Kim, Y. H.; Kim, J. C.; Huh, W.; Lee, J.; Park, S.; Jeong, H. Y.; Kim, Y. D.; Lee, C.-H. Remote modulation doping in van der Waals heterostructure transistors. *Nat. Electron.* **2021**, *4*, 664−670.

(24) Cai, L.; McClellan, C. J.; Koh, A. L.; Li, H.; Yalon, E.; Pop, E.; Zheng, X. Rapid Flame Synthesis of Atomically Thin MoO_3 down to Monolayer Thickness for Effective Hole Doping of WSe2. *Nano Lett.* **2017**, *17*, 3854−3861.

(25) Joo, M.-K.; Moon, B. H.; Ji, H.; Han, G. H.; Kim, H.; Lee, G.; Lim, S. C.; Suh, D.; Lee, Y. H. Electron Excess Doping and Effective Schottky Barrier Reduction on the MoS_2/*h*-BN Heterostructure. *Nano Lett.* **2016**, *16*, 6383−6389.
(26) Wang, F.; Tu, B.; He, P.; Wang, Z.; Yin, L.; Cheng, R.; Wang, J.; Fang, Q.; He, J. Uncovering the Conduction Behavior of van der Waals Ambipolar Semiconductors. *Adv. Mater.* **2019**, *31*, 1805317.
(27) Wang, Y.; Chhowalla, M. Making clean electrical contacts on 2D transition metal dichalcogenides. *Nat. Rev. Phys.* **2022**, *4*, 101−112.
(28) Naguib, M.; Mochalin, V. N.; Barsoum, M. W.; Gogotsi, Y. 25th Anniversary Article: MXenes: A New Family of Two-Dimensional Materials. *Adv. Mater.* **2014**, *26*, 992−1005.
(29) Liu, Y.; Xiao, H.; Goddard, W. A. Schottky-Barrier-Free Contacts with Two-Dimensional Semiconductors by Surface-Engineered MXenes. *J. Am. Chem. Soc.* **2016**, *138*, 15853−15856.
(30) Naguib, M.; Halim, J.; Lu, J.; Cook, K. M.; Hultman, L.; Gogotsi, Y.; Barsoum, M. W. New Two-Dimensional Niobium and Vanadium Carbides as Promising Materials for Li-Ion Batteries. *J. Am. Chem. Soc.* **2013**, *135*, 15966−15969.
(31) Zhou, J.; Zha, X.; Zhou, X.; Chen, F.; Gao, G.; Wang, S.; Shen, C.; Chen, T.; Zhi, C.; Eklund, P.; Du, S.; Xue, J.; Shi, W.; Chai, Z.; Huang, Q. Synthesis and Electrochemical Properties of Two-Dimensional Hafnium Carbide. *ACS Nano* **2017**, *11*, 3841−3850.
(32) Gong, C.; Colombo, L.; Wallace, R. M.; Cho, K. The Unusual Mechanism of Partial Fermi Level Pinning at Metal−MoS_2 Interfaces. *Nano Lett.* **2014**, *14*, 1714−1720.
(33) Lin, T.; Kang, B.; Jeon, M.; Huffman, C.; Jeon, J.; Lee, S.; Han, W.; Lee, J.; Lee, S.; Yeom, G.; Kim, K. Controlled Layer-by-Layer Etching of MoS_2. *ACS Appl. Mater. Interfaces* **2015**, *7*, 15892−15897.
(34) Lee, D.; Choi, Y.; Kim, J.; Kim, J. Recessed-Channel WSe_2 Field-Effect Transistor via Self-Terminated Doping and Layer-by-Layer Etching. *ACS Nano* **2022**, *16*, 8484−8492.
(35) Di Valentin, C.; Palma, G.; Pacchioni, G. Ab Initio Study of Transition Levels for Intrinsic Defects in Silicon Nitride. *J. Phys. Chem. C* **2011**, *115*, 561−569.

https://doi.org/10.1021/acs.nanolett.2c04011
Nano Lett. 2022, 22, 9700−9706